Tipping the Balance with the Aid of Stoichiometry: Room Temperature Phosphorescence versus Fluorescence in Organic Cocrystals

Tipping the balance with the aid of stoichiometry: Room temperature phosphorescence vs fluorescence in organic co-crystals.

Simone d'Agostino,[a,*] Fabrizia Grepioni,[a] Dario Braga,[a] Barbara Ventura[b,*]

[a] Dipartimento di Chimica "Giacomo Ciamician", Università di Bologna, Via F. Selmi, 2, 40126 Bologna, Italy.

[b] Istituto ISOF-CNR, Via P. Gobetti, 101, 40219 Bologna, Italy.

KEYWORDS mechano, stoichiometry, organic, heavy atom effect, photophysics

ABSTRACT: The interaction of the co-former 1,4-diiodotetrafluorobenzene (I_2F_4) with the conjugated hydrocarbons diphenylacetylene (DPA) and ~~trans-~~*trans*-stilbene (tS) leads to formation of the novel co-crystals DPA·I_2F_4 (**1**), DPA·$(I_2F_4)_2$ (**2**), tS·I_2F_4 (**3**), and tS·$(I_2F_4)_2$ (**4**). These materials have been synthesized by mechanochemical methods and characterized by X-ray techniques and luminescence spectroscopy in the solid state. In the co-crystals, the DPA and tS molecules interact with the molecules of I_2F_4 *via* halogen bonds (XB) of the kind halogen···phenyl (Hlg···π). As a result of the external heavy atom effect, and depending on the stoichiometry, these co-crystals exhibit both fluorescence and phosphorescence (**1** and **3**) or exclusive phosphorescence (**2** and **4**) at room temperature. Differences in the luminescence efficiencies between the DPA- and tS-containing materials are observed.

INTRODUCTION

Wholly organic compounds able to display luminescence, with good yields in the solid state,[1] have attracted significant interest for their potential applications in light-emitting diodes,[2] solid state lasers[3] and nonlinear optoelectronic devices.[4] Recently, the interest in obtaining phosphorescence from purely organic solid compounds, which compared to fluorescence is a more rarely observed phenomenon, has emerged.[5, 6]

A novel and promising approach for controlling the optical features of emitting molecules, in the solid-state, comes from crystal engineering,[7] which aims to modify the solid-state properties through a careful control of the interactions that lead to the assembly of the components into the final solid.

Within this strategy, co-crystallization of organic units with halogenated co-formers has proved to be successful in lighting up phosphorescence.

This approach is based on co-crystal formation via halogen bonds (XB)[8] and makes use of organic co-formers containing heavy atoms, as they play two main roles inside the co-crystals: (1) they serve as solid diluents to prevent the emitting molecule from aggregating and self-quenching, and (2) they act as perturbants and induce phosphorescence emission in the organic chromophore through an external heavy atom effect.[6,9]

But two aspects have not been explored yet, namely i) the possibility of obtaining this class of compounds via mechanochemistry and ii) the understanding of how the perturbant:organic emitter ratio affects the luminescence properties of the final solid.

With this questions in mind, we have chosen two compounds well known for their photophysics, namely diphenylacetylene (DPA), and ~~trans-~~*trans*-stilbene (tS), which not only are, due to their unique properties, a kind of milestone in photochemistry, but they are also promising materials for solid state lighting applications. Despite their low fluorescence in solution, due to the fast depletion of the emissive singlet excited state through the population of accessible states with distorted geometry,[10] they are known to be highly emissive in the solid state, and crystals of DPA and tS and have been intensely studied as scintillators.[11] Although most of the solid state applications of DPA and tS are based on fluorescence emission recent reports document the observation of DPA phosphorescence in crystals and in adducts with organomercurials.[12] Here we report on the structural and photophysical characterization of four novel co-crystals of formula: DPA·I_2F_4 (**1**), DPA·$(I_2F_4)_2$ (**2**), tS·I_2F_4 (**3**), and tS·$(I_2F_4)_2$ (**4**) which have been synthesized directly in the solid-state through mechanochemical methods and then further characterized by means of XRD techniques and steady-state and time-resolved luminescence techniques. This study gives new insights into the relationship between stoichiometric ratio (organic emitter/co-former) and photophysical properties (fluorescence/phosphorescence) of organic co-crystals obtained *via* mechanochemical methods.

EXPERIMENTAL SECTION

All solvents and chemicals were bought from Sigma-Aldrich and used without further purification. Prior to be employed in the synthesis of co-crystals, commercial diphenylacetylene (DPA) and ~~trans-~~*trans*-stilbene (tS) were subjected to powder x-Ray diffraction analysis and identified by comparing the experimental patterns with those calculated from the crystal structure extracted from the Cambridge Structural Database (reference codes are DPHACTo8 and TSTILBo4, respectively, see SI for PxRD patterns).

Solid-state synthesis. Co-crystals DPA·I2F4 (**1**), DPA·$(I2F4)_2$ (**2**), tS·I2F4 (**3**), and tS·$(I2F4)_2$ (**4**) have been synthesized, in the solid state, according to scheme 1.

Scheme 1. Synthetic route to co-crystals with: (a) DPA [DPA·I2F4 (1) and DPA·$(I2F4)_2$ (2)] and, (b) with tS [tS·I2F4 (3) and tS·$(I2F4)_2$ (4)]. I2F4 = 1,4-diiodotetrafluorobenzene; DPA = diphenylacetylene; tS = *trans*-stilbene. All reactions were performed in the solid state.

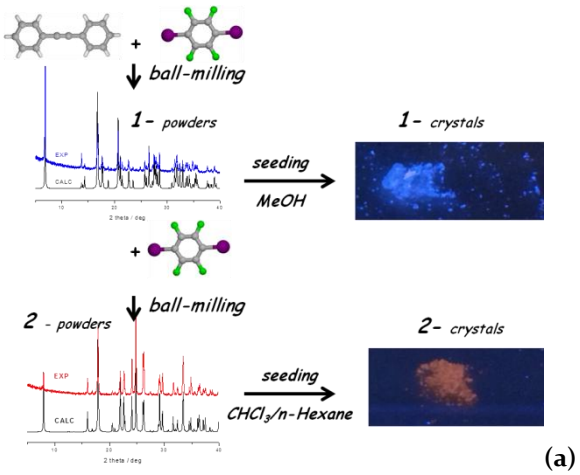

Ball-milling and Crystallization Experiments. 1,4-diiodotetrafluorobenzene (I2F4) and diphenylacetylene (DPA) or *trans*-stilbene (tS) were weighed in 1:1 molar ratio (total maximum amount was around 200 mg) and ground together for 90 min in a ball-milling apparatus Retsch MM 20 operated at 15 Hz. The solid products were divided in two portions. One was employed to grow single crystals via seeding[13] in methanol; the other one was first analyzed by XRPD, then further reacted, in the same mechanical conditions, with an additional equivalent of I2F4. The new products were divided again in two portions: the first was characterized by XRPD analysis, while the second was employed to grow single cystals via seeding in $CHCl_3$ / n-Hexane 4: 1. Co-crystals formation was confirmed by comparison of the experimental XRPD patterns with those calculated on the basis of single crystal data. ATR-FTIR spectra were recorded for all co-crystals (see SI).

IR spectroscopy. The attenuated total reflectance Fourier transform IR (ATR-FTIR) spectra were obtained using a Bruker Alpha FT-IR spectrometer.

Crystal structure determination. Single-crystal data for all co-crystals were collected at RT on an Oxford X'Calibur S CCD diffractometer equipped with a graphite monochromator (Mo-Kα radiation, λ = 0.71073Å). Data collection and refinement details are listed in Table 1. The structure of **4** is affected by positional disorder of the ~~trans-~~*trans*-stilbene. All non-hydrogen atoms, with exception of those of the double bond of the *trans*-stilbene in **4**, were refined anisotropically; HCH atoms for all compounds were added in calculated positions and refined riding on their respective carbon atoms. SHELX97[14a] was used for structure solution and refinement on F^2. The program Mercury[14b] was used to calculate intermolecular interactions. CYLview[14c] and Mercury[14b] were used for molecular graphics. The tS molecule in **4** is affected by disorder. This fact is not surprising, as in crystal structures containing stilbene-like molecules an orientational disorder can be observed associated also with a pedal motion;[15] molecules frequently adopt, as in this case, two conformations related by a 2-fold rotation about the longest molecular axis (see SI). Crystal data can be obtained free of charge via www.ccdc.cam.ac.uk/conts/retrieving.htmL (or from the Cambridge Crystallographic Data Centre, 12 Union Road, Cambridge CB21EZ, UK; fax: (+44)1223-336-033; or e-mail: deposit@ccdc.cam.ac.uk).

Powder diffraction measurements. X-ray powder diffractograms in the 2θ range 5-40° (step size, 0.02°; time/step, 20 s; 0.04 rad soller; 40mA x 40kV) were collected on a Panalytical X'Pert PRO automated diffractometer equipped with an X'Celerator detector and in Bragg-Brentano geometry, using Cu Kα radiation without a monochromator. The program Mercury[14b] was used for simulation of X-ray powder patterns on the basis of single crystal data. Chemical and structural identity between bulk materials and single crystals was always verified by

comparing experimental and simulated powder diffraction patterns.

Table 1. Crystallographic data and details of measurements for co-crystals: DPA·I2F4 (1), DPA·(I2F4)2 (2), tS·I2F4 (3), and tS·(I2F4)2 (4).

	1	2	3	4
Formula	$C_{20}H_{10}F_4I_2$	$C_{26}H_{10}F_8I_4$	$C_{20}H_{12}F_4I_2$	$C_{26}H_{12}F_8I_4$
fw	580.08	981.94	582.10	983.96
Cryst. System	Monoclinic	Monoclinic	Monoclinic	Monoclinic
Space group	$P2_1/c$	C2/c	$P2_1/c$	C2/c
Z	2	4	2	4
a (Å)	13.134(1)	22.1118(6)	13.250(2)	22.549(5)
b (Å)	5.7484(5)	14.3288(4)	5.7590(7)	14.166(5)
c (Å)	12.899(1)	8.6508(2)	12.691(2)	8.650(5)
α (deg)	90	90	90	90
β (deg)	101.080(8)	90.657(2)	101.300(1)	91.442(5)
γ (deg)	90	90	90	90
V (Å^3)	955.71(15)	2740.70(12)	949.7(2)	2762(2)
D_{calc} (g/cm^3)	2.016	2.380	2.036	2.366
μ (mm^{-1})	3.328	4.617	3.349	4.582
Measd reflns	6970	10732	4114	6385
Indep reflns	2291	3293	2173	3158
R_1[on Fo^2, $I>2\sigma(I)$]	0.0354	0.0483	0.0733	0.0622
wR_2 (all data)	0.0680	0.0888	0.1486	0.1381

Photophysics. All the measurements were performed on uncrushed powder samples placed inside two quartz slides, or in quartz capillary tubes immersed in liquid nitrogen in a cold finger quartz Dewar, for room temperature and 77K determinations, respectively.

Steady-state emission spectra were collected in front-face mode with an Edinburgh FLS920 fluorimeter equipped with a Peltier-cooled Hamamatsu R928 PMT (200-850 nm), and corrected for the wavelength dependent phototube response. Absolute emission quantum yields were determined according to the method reported by Ishida et al.,[16] by using a 6 inches Labsphere integrating sphere. Each measurement was repeated from three to ten times. The limit of detection of the system is 0.020.

Gated emission spectra were acquired in front-face mode with the same fluorimeter by using a time-gated spectral scanning mode and a μF920H Xenon flash lamp (pulse width < 2 μs, repetition rate between 0.1 and 100 Hz) as excitation source. Spectra were corrected for the wavelength dependent phototube response. Luminescence decays in the μs-ms regime were measured with the same apparatus in multi-channel scaling mode. For weak signals the measurements were repeated from four to five times.

Fluorescence lifetimes were determined with an IBH 5000F time-correlated single-photon counting apparatus by using a pulsed NanoLED excitation source at 331 nm. Analysis of the luminescence decay profiles against time was accomplished with the Decay Analysis Software DAS6 provided by the manufacturer. The estimated error on lifetime determination is 10%.

RESULTS AND DISCUSSION

Crystal structure description. X-ray single crystal structural analysis revealed that stoichiometry of conjugated hydrocarbons (DPA or tS) to the co-former 1,4-diiodotetrafluorobenzene (I2F4) is 1:1 for the pair DPA·I2F4 (**1**), and tS·I2F4 (**3**) and 1:2 for DPA·$(I2F4)_2$ (**2**), and tS·$(I2F4)_2$ (**4**). All co-crystals are characterized by the presence of Hlg···π interactions[8] (see Figure 1 and Table 2).

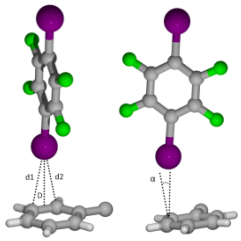

FIGURE 1. Geometry of the C–I···π interactions observed in crystalline 1-4, and geometric parameters, reported in Table 2, used for the halogen···phenyl description and for the evaluation of the hapticity (η). d1 and d2 refer to the distances between the halogen atom and the nearest two carbon atoms in the aromatic ring (d1< d2), D refers to the shortest distance between the halogen atom and the C–C bond on the 6-membered ring, and α is the angle between the C—I bond and the normal to the aromatic ring.

Table 2. Geometric parameters used to evaluate the XB found in co-crystals 1, 2, 3, and 4.

	d1 (Å)	d2 (Å)	D (Å)	α (°)	η
DPA·I2F4 (**1**)	3.479(4)	3.544(4)	3.443(1)	7.39	1.82
DPA·$(I2F4)_2$ (**2**)	3.520(6)	3.542(5)	3.465(2)	11.2	1.91
	3.573(6)	3.633(6)	3.539(1)	10.15	1.74
tS·I2F4 (**3**)	3.511(2)	3.581(2)	3.477(1)	7.10	1.79
tS·$(I2F4)_2$ (**4**)	3.588(2)	3.627(4)	3.547(2)	12.37	1.97
	3.482(8)	3.528(2)	3.443(1)	3.14	1.92

In all cases, we found that the I2F4 molecule is oriented almost perpendicularly and at short distance to the DPA

or tS aromatic rings. By analogy with organometallic compounds, we can describe this interaction as an η^2 (η = hapticity, η^2 = over-bond coordination). This is in a good agreement with the results on analogous compounds, formerly reported by Wei Jun Jin and co-workers,[6] and provides additional evidence on how halogen atoms interact with π-systems.

The pairs **1**, **3** and **2**, **4** will now be discussed together, for sake of clarity, since their structures were found to be isomorphous.

For crystalline **1** and **3** the overall packing is made of alternating layers of molecules (DPA or tS) and co-formers, see Figure 2. It is worth noting that the packing strongly resembles the one observed for pure DPA and tS (CSD refcode are DPHACT08, and TSTILB04, respectively), as it shown in Figure 2. The two co-crystals can be seen as intercalation solids, where the I_2F_4 molecules replace alternating layers of DPA or tS molecules in the parent crystals. Therefore the C-I···π interactions in the **1** and **3** systems are more relevant than the C—H···π interactions observed in pure DPA and tS crystals (see Figure 3).

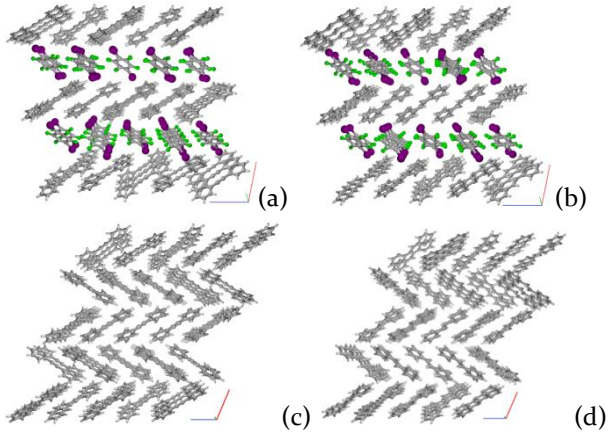

Figure 2. Ball and stick representations of crystalline **1** (a) and **3** (b) viewed along the b-axis: it is evident how alternate layer of DPA or tS molecules in the pure parent crystals (c) and (d) are replaced by I_2F_4 layers in the **1** (a) and **3** (b) co-crystals.

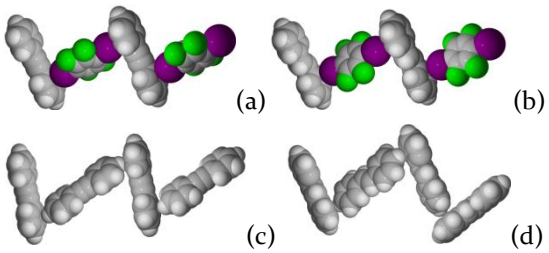

Figure 3. Space filling representation of the 1D chevron-like arrangement in crystalline 1 (a) and 3 (b), where C-I···π interactions take the place of C-H···π interactions in pure DPA (c) and tS (d) crystals.

On changing the DPA/tS : I_2F_4 stoichiometry from 1:1 to 1:2, the co-crystals DPA· $(I_2F_4)_2$ (2), and tS·$(I_2F_4)_2$ (4) are obtained, which present markedly different packing features.

As can be seen in Figure 6, in both co-crystals DPA or tS and I_2F_4 molecules are arranged in a 2D network, in which the building blocks are held together via C-I···π interactions.

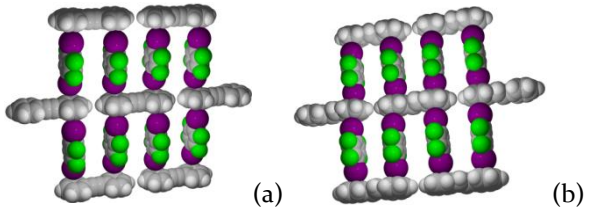

Figure 6. Space filling representation of the 2D C-I···π networks in crstalline **2** (a) and **4** (b). Only one of the two possible orientations of the tS molecule is shown for **4**.

As observed for crystalline **1** and **3**, also co-crystalline **2** and **4** can be seen as formed by an alternating sequence of DPA or tS molecules and co-formers, although in these crystals the relative arrangement within the single layers is different, as it can be seen in Figure 7.

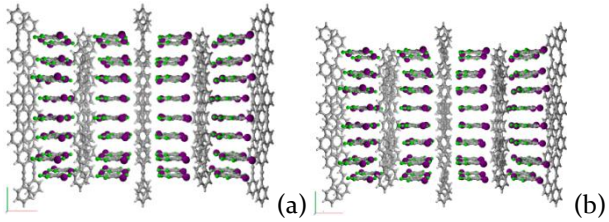

Figure 7. Crystal packing (projection along the c-axis), for co-crystals **2** and **4**, highlighting the layered structure in which DPA or tS layers alternate to I_2F_4 layers. For compound **4** is shown only one of the two possible orientations of tS molecules.

We tried to prepare pure samples of the co-crystals by solution methods, but all attempts failed since the reaction was never quantitative, making the resulting polycrystalline solids unsuitable for photophysical characterization. To circumvent these drawbacks, a solvent-free mechanochemical approach was employed to produce co-crystals. Grinding was carried out by means of an automated ball-milling apparatus (see experimental section for details, and Figure S5 for the X-ray powder patterns of the solid products). The co-crystals thus obtained were recrystallized *via* seeding of a methanol solution or of a chloroform/n-hexane (4:1) solution for the 1:1 (**1** and **3**) and 1:2 (**2** and **4**) co-crystals, respectively (see Figure S6 for for X-ray powder patterns). Recrystallized samples were then used for the photophysical characterization

Photophyscical Characterization. The photophysical properties of the four co-crystals **1**-**4** have been examined in the solid state both at room temperature and at 77K, and compared with those of the relevant models DPA and tS as pure crystals. The room temperature and 77K data are collected in Table 3 and Table S1, respectively.

Room temperature emission. Solid DPA and tS both show an intense fluorescence emission at room temperature, peaking at 358 nm and 366 nm respectively, with quantum yield close to unit and lifetime in the ns regime (Table 3). The observed fluorescence spectral features are in agreement with literature,[11a,11c] whereas the measured emission quantum yields are higher than those previously reported (ϕ_{fl} = 0.65-0.77 for tS single crystals or powders),[17] likely due to the unmilled, small single crystal nature of the present samples.

Table 3. Luminescence data at room temperature.

	λ_{fl}^{max} / nm	τ_{fl} / ns	λ_{phos}^{max} / nm	τ_{phos} / ms	ϕ_{em}
DPA	358, 376, 398sh	1.46	568, 620	0.85 (65%); 3.53 (35%)	0.990 ± 0.066
1	358, 376, 398sh	< 0.20	580, 634, 698, 774sh	3.55	0.167 ± 0.044
2	-	-	578, 634, 698, 770	0.70	0.057 ± 0.002
tS	366, 379, 407sh	0.77 (40%); 7.70 (60%)	-	-	0.939 ± 0.048
3	370, 379[a]	< 0.20	580, 634, 686, 756	0.23[b]	0.007 ± 0.001[c]
4	380[a]	< 0.20	582, 638, 700, 768	0.12[b]	0.008 ± 0.001[c]

[a] Weak signal. [b] Reported as weighted average lifetimes from two exponentials because of the weakness of the signal. [c] Below instrumental resolution (0.020).

The luminescence features of co-crystals **1** and **2** are significantly different from those of pure DPA (Figure 8 and Table 3). Co-crystal **1** shows a weak fluorescence emission accompanied by weak but clear phosphorescence with maxima at 580, 634 and 698 nm, whereas in co-crystal **2** the fluorescence is completely suppressed and only phosphorescence is observed. Phosphorescence spectra of the two co-crystals are evidenced upon pulsed excitation and gated detection (Figure S7). The spectral features are almost identical but the phosphorescence lifetime of **2** is much shorter than that of **1** (700 μs vs 3.55 ms, Table 3), due to the increased $T_1 \rightarrow S_0$ radiative deactivation rate induced by the doubled heavy atom:DPA stoichiometry in the co-crystal. It can be noted that the 0-0 vibronic band of the phosphorescence spectrum of **1** and **2** is largely red-shifted with respect to DPA phosphorescence registered at low temperature in solution or in PMMA film (0-0 band at 450-470 nm).[18,19] Moreover the spectrum is unusually dominated by a marked vibronic progression of ca. 1450 cm^{-1} (Figures 8 and S7 and Table 3), at variance with DPA phosphorescence in frozen solution which shows weak vibronic features originated by both C≡C stretching (2200 cm^{-1}) and total symmetric vibrations (1130 and 1580 cm^{-1}).[18] Similar phosphorescence spectra have been observed for DPA-fluorinated organomercurial adducts,[12a] indicating that an external heavy atom packed in the solid lattice, in addition to the perturbation of the spin-orbit coupling, affects the nature and the energy of the triplet state. Interestingly, also pure DPA shows a structured emission clearly detectable in gated mode (Figure 7), weak but visible even upon continuous excitation (Figure 8), peaking at 568 nm and with lifetime in the ms regime (Table 3). The long lifetime accounts for phosphorescence, but the energy of the transition is much lower compared to a recently reported crystallization-induced phosphorescence from DPA crystals.[12b] We tentatively ascribe it to an aggregated form of DPA in the solid, supported by the presence of a low energy shoulder in the excitation spectrum (Figure S8). It can be pointed out that the luminescence spectrum of **1** is still dominated by fluorescence with an overall emission quantum yield of ca. 0.17, i.e. about one sixth that of model DPA, indicative of an effective promotion of intersystem crossing induced by the halogenated co-former, whereas the 2:1 (co-former:DPA) stoichiometry of **2** renders intersystem crossing the dominating process, with the result of sole phosphorescence with a considerable quantum yield of 0.057. Excitation spectra collected on fluorescence and phosphorescence regions of the three compounds (Figure S8) reveal that DPA absorption in **2** is red-shifted and broadened with respect to pure DPA and **1**, indicating a perturbation likely induced by the higher co-former stoichiometry and/or by the different DPA network in the crystal.

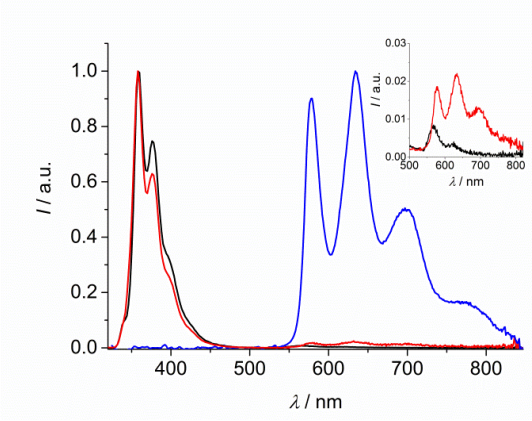

Figure 8. Normalized corrected emission spectra of DPA (black), **1** (red) and **2** (blue) in the solid state at room

temperature, λ_{exc} = 315 nm. Spectral portions in the 500-800 nm region are magnified in the inset for DPA and **1**.

tS containing co-crystals **3** and **4** display a luminescence behavior similar to that observed for co-crystals **1** and **2**, but with relevant differences in terms of emission efficiencies. In both **3** and **4** the tS fluorescence is nearly completely quenched, with a short lived residual emission around 370 nm, more evident in **3** (Figure 9 and Table 3). Almost only phosphorescence is detected but with a very low emission quantum yield, measured at the limit of our instrumental resolution (see Table 3). Phosphorescence spectra isolated with the gated mode, are shown in Figure S8. The lifetimes are rather short, of the order of 200 μs and 100 μs for **3** and **4** respectively (Table 3), the shorter lifetime of **4** explained by stoichiometry. Overall, the behavior indicates that in the case of tS the 1:1 (tS:co-former) ratio is already efficiently promoting both intersystem crossing and phosphorescence rate and the role of stoichiometry is less important than for DPA. This effect, though leading to the interesting achievement of purely phosphorescent materials with low heavy atom content has the drawback of making phosphorescence weak. The phosphorescence spectrum in this case matches that observed for tS at low temperature in different matrices.[20,21,22,23] To the best of our knowledge this is the first report of tS phosphorescence registered at room temperature. Excitation spectra (Figure S10) indicate a perturbation effect in **4** similar to that noted in **2**.

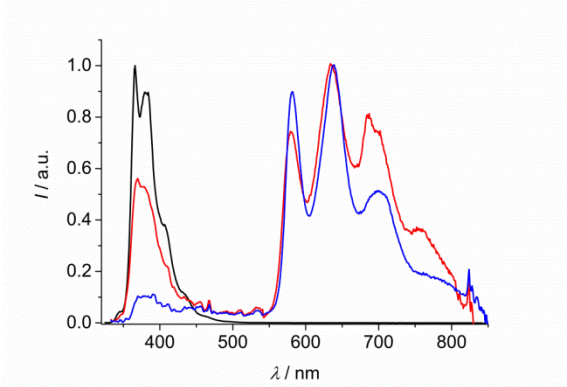

Figure 9. Normalized corrected emission spectra of tS (black), **3** (red) and **4** (blue) in the solid state at room temperature, λ_{exc} = 315 nm.

Low temperature emission. The luminescence features of the two series at 77K reproduce the behavior observed at room temperature, with the peculiarity of an increased spectral resolution of both fluorescence and phosphorescence bands.

DPA shows a bright fluorescence peaking at 359 nm, accompanied by a long-lived emission in the 550-750 nm region (Figure S11, Table S1). Co-crystal **1** mainly shows fluorescence together with a weak but discernable phosphorescence, while co-crystal **2** displays only triplet emission, peaking at 572 nm (Figures S11 and S12). The phosphorescence lifetimes, though longer than those measured at room temperature, follow the same trend (Table S1).

In the tS co-crystals, the intense tS fluorescence is suppressed and both **3** and **4** emit weakly, with co-crystal **3** exhibiting a faint phosphorescence anomalously red-shifted compared to **4** (Figures S13 and S14). Phosphorescence lifetimes, of the order of hundreds of μs, are in line with room temperature data (Table S1).

Overall the similarity between the luminescence features at the two temperatures confirm that co-crystals are ideal constrained systems that prevent diffusion-controlled quenching phenomena, thus enabling the modulation of the photophysical properties at room temperature solely by playing on the stoichiometry.

Conclusions

Four new co-crystals, namely DPA·I_2F_4 (**1**), DPA·$(I_2F_4)_2$ (**2**), tS·I_2F_4 (**3**), and tS·$(I_2F_4)_2$ (**4**) were prepared by co-grinding the components in a ball-milling apparatus.

Crystal structures of all of these species were solved from single-crystals obtained via seeding which also allowed to obtain polycrystalline specimens suitable for photophysical characterization.

The luminescence properties of the co-crystals in the solid state were studied and compared with those of pure DPA and tS crystals. The bright fluorescence of the model crystals was found to be greatly reduced in all the co-crystals. For DPA the 1:1 stoichiometry leads to a dual luminescent material which exhibits both fluorescence and phosphorescence emission. The 1:2 product, instead, is a pure triplet emitter, with a phosphorescence quantum yield at room temperature of the order of 0.06. Co-crystals **3** and **4** behave similarly but with an overall weaker emission. The results prove the principle of tuning between fluorescence and phosphorescence in organic materials by acting on the co-crystal stoichiometry, opening the way to new strategies in the field.

ASSOCIATED CONTENT

Supporting Information. X-ray powder patterns for DPA, tS and co-crystals as obtained by grinding processes and after seeding Ortep drawings and CIF files for compounds **1–4**.Emission and excitation spectra of DPA, tS, and co-crystals at RT and at 77K. This material is available free of charge via the Internet at http://pubs.acs.org.

AUTHOR INFORMATION

Corresponding Authors

* E-mail address: simone.dagostino2@unibo.it
* E-mail address: barbara.ventura@isof.cnr.it

Author Contributions

The manuscript was written through contributions of all authors.

Funding Sources

Any funds used to support the research of the manuscript should be placed here (per journal style).

Notes

The authors declare no competing financial interest

ACKNOWLEDGMENT

CNR (Project PM.P04.010 "MACOL"), MIUR project PRIN 2010CX2TLM, MIUR-CNR project Nanomax N-CHEM and the University of Bologna are gratefully acknowledged.

ABBREVIATIONS

DPA, diphenylacetylene; tS, *trans*-stilbene; I2F4, 1,4-diiodotetrafluorobenzene.

REFERENCES

(1) (a) Wuest, J. D. *Nat. Chem.* **2012**, *4*, 74–75. (b) Shimizu, H. *Chem. Asian J.* **2010**, *5*, 1516 – 1531. (c) Anthony, S. P. *ChemPlusChem* **2012**, *77*, 518-531. (d) Anthony, S. P.; Varughese, S.; Draper, S. M. *Chem. Commun.* **2009**, *48*, 7500- 7502.

(2) (a) Shi, H.; Xin, D.; Dong, X.; Dai, J.-X.; Wu, X.; Miao, Y.; Fang, L.; Wang, H.; Choi, M. M. M F. *J. Mater. Chem. C* **2014**, *2*, 2160–2168. (c) Friend, R. H.; Gymer, R. W.; Holmes, A. B.; Burroughes, J. H.; Marks, R. N.; Taliani, C.; Bradley, D. D. C.; Dos Santos, D. A.; Brédas, J. L.; Lögdlund, M.; Salaneck, W. R. *Nature*, **1999**, *397*, 121–128. (d) Wei, Y.; Wang, W.-J.; Huang, Y.-T.; Wang, B.-C.; Chen, W.-H.; Wua, S.-H.; He, C.-H.; *J. Mater. Chem. C* **2014**, *2*, 1779–1782. (f) Lee, C. W.; Lee, J. Y. *Chem. Mater.* **2014**, *26*, 1616–1621.

(3) (a) Samuel, D. W.; Turnbull, G. A. *Chem. Rev.* **2007**, *107*, 1272-1295. (b) McGehee, M. D.; Heeger, A. *J. Adv. Mater.* **2000**, *22*, 1655-1668.

(4) (a) Gao, F.; Liao, Q.; Xu; Z-Z.; Yue, Y.-H.; Wang, Q.; Zhang, H.-L.; Fu, H.-B. *Angew. Chem. Int. Ed.* **2010**, *49*, 732 –735; (b) Botta, C.; Cariati, E.; Cavallo, G.; Dichiarante, V.; Forni, A.; Metrangolo, P.; Pilati, T.; Resnati, G.; Righetto, S.; Terraneo, G.; Tordin, E. *J. Mater. Chem. C* **2014**, *2*, 5275–5279

(5) (a) Bolton, O.; Lee, K.; Kim, H.-J.; Lin, K. Y.; Kim, J.; *Nat. Chem.* **2011**, *3*, 205–210. (b) Bolton, O.; Lee, D.; Jung, J.; Kim, J.; *Chem. Mater.* **2014**, *26*, 6644–6649.

(6) (a) Pang, X.; Wang, H.; Zhao, X. R.; Jin, W. J. *CrystEngComm* **2013**, *15*, 2722-2730. (b) Shen, Q. J.; Pang, X.; Zhao, X. R.; Gao, H. Y.; Sun, H-L.; Jin, W. J. *CrystEngComm* **2012**, *14*, 5027-5034. (c) Shen, Q. J.; Wei, H. Q.; Zou, W. S.; Sun, H. L.; Jin, W. J. *CrystEngComm* **2012**, ***14***, 1010-1015. (d) Gao, H. Y.; Zhao, X. R.; Wang, H.; Pang, X.; Jin, W. J. *Cryst. Growth Des.* **2012**, *12* , 4377–4387.

(7) (a) Braga, D.; Grepioni, F.; Orpen, A. G. in *Crystal Engineering: from Molecules and Crystal to Materials*, Kluwer Academic Publishers, Dordrecht, **1999**. (b) Aakeröy, C. B.; Champness, N. R.; Janiak, C. *CrystEngComm* **2010**, *12*, 22–43. (c) Mizobe, Y.; Hinoue, T.; Yamamoto, A.; Hisaki, I.; Miyata, M.; Hasegawa, Y.; Tohnai, N. *Chem. Eur. J.* **2009**, *15*, 8175-8184.

(8) (a) Metrangolo, P.; Murray, J. S.; Pilati, T.; Politzer, P.; Resnati, G.; Terraneo, G. *Cryst. Growth Des.* **2011**, *11*, 4238–4246. (b) Politzer, P.; Murray, J. S.; Clark, T. Phys. *Chem. Chem. Phys.* **2010**, *12*, 7748– 7757. (c) Desiraju, G. R.; Ho, P. S., Kloo, L.; Legon, A. C.; Marquardt, R.; Metrangolo, P.; Politzer, P.; Resnati, G.; Rissanen, K. *Pure Appl. Chem.* **2013**, *8*, 1711–1713.

(9) Ventura, B.; Bertocco, A.; Braga, D.; Catalano, L.; d'Agostino, S.; Grepioni, F.; Taddei, P. *J. Phys. Chem. C* 2014, *118*, 18646–18658.

(10) (a) Saltiel, J.; D'Agostino, J. T. *J. Am. Chem. Soc.***1972**, *18*, 6445-6456. (b) Whitten, D. G . *Acc. Chem. Res.* **1993**, *26*, 502-509. (c) Charlton, J. L.; Saltlel, J. *J. Phys. Chem.* **1977**, *20*, 1940-**1944**. (d) Semionova, V. V. ; Glebov, E. M.; Korolev, V. V. ; Sapchenko, S. A.; Samsonenko, D. G.; Fedin, V. P. *Inorg. Chim. Acta* **2014**, *409*, 342–348 (e) Zgierski, M. Z.; Lim, E. C.; *Chem. Phys. Letters* **2004**, *387*, 352–355 (f) Menning, S.; Krämer, M.; Duckworth, A.; Rominger, F.; Beeby, A.; Dreuw, A.; Bunz, U. H. F. *J. Org. Chem.* **2014**, *79*, 6571–6578.

(11) (a) Birks, J. B.; Wright, G. T. *Proc. Phys. Soc. B* **1954**, *67*, 657-663. (b) Birks, J.B. *Phys. Rev.* **1954**, *6*, 1567-1573. (c) Zaitseva, N.; Newby, J.; Hamel, S.; Carman, L.; Faust, M.; Lordi, V.; Cherepy, N.; Stoeffl, W.; Payne S. *SPIE Hard X-Ray, Gamma-Ray, and Neutron Detector Physics XI* **2009**.

(12) Taylor, T.J.; Elbeirami, O.; Burress, C. N.; Tsunoda, M.I.; Omary, M. A.; Gabbai, F. P. *J. Inorg. Organomet. Polym.* **2008**, *18*, 175–179. (b) Hong, Y.; Lam, J. W. Y.; Zhong Tang, B. *Chem. Commun.* **2009**, 4332–4353. (c) Carman, L.; Zaitseva, N.; Martinez, H. P.; Rupert, B.; Pawelczak, I.; Glenn, A.; Mulcahy, H.; Leif, R.; Lewis, K.; Payne, S. *J. Cryst. Growth* **2013**, *368*, 56–61. (d) Zaitseva, N.; Glenn, A.; Carman, L.; Hatarik, R.; Hamel, S.; Faust, M.; Schabes, B.; Cherepy, N.; Payne, S. *IEEE Trans. On Nucl. Science* **2011**, *6*, 3411-3420. (e) Hull, G.; Zaitseva, N.; Cherepy, J.; Newby, J. R.; Stoeffl, W.; Payne, S. A. *IEEE Trans. On Nucl. Science* **2009**, *3*, 899-903.

(13) Khurshid, S.; Haireb, L. F.; Chayen, N. E. J. Appl. Cryst. **2010**, 43, 752–756.

(14) (a) Sheldrick, G. M. SHELX97, Program for Crystal Structure Determination; University of Göttingen: Göttingen, Germany, **1997**. (b) Speck, A. L. PLATON; *Acta Crystallogr., Sect. A* **1990**, 46, C34. (c) Legault, C. Y. CYLview, Université de Sherbrooke, **2009**. (d) Macrae, C. F.; Bruno, I. J.; Chisholm, J. A.; Edgington, P. R.; McCabe, P.; Pidcock, E.; Rodriguez-Monge, L.; Taylor, R.; van de Streek, J.; Wood, P. A. *J. Appl. Crystallogr.* **2008**, 41, 466–470.

(15) (a) Harada, J.; Ogawa, K. *Chem. Soc. Rev.* **2009**, *38*, 2244–2252. and references cited therein. (b) Harada, J.; Ogawa, K. *J. Am. Chem. Soc.* **2001**, *123*, 10884-10888. (c) Galli, S. Mercandelli, P.; Sironi, A. *J. Am. Chem. Soc.* **1999**, *121*, 3767-3772.

(16) Ishida, H.; Tobita, S.; Hasegawa, Y.; Katoh, R.; Nozaki, K. *Coord. Chem. Rev.* **2010**, *254*, 2449-2458.

(17) (a) Katoh, R.; Suzuki, K.; Furube, A.; Kotani, M.; Tokumaru, K. *J. Phys. Chem.* C **2009**, *113*, 2961–2965. (b) Tarasenko, O.A.; Galunov, N.Z.; Panikarskaya, V.D.; Sanin, E.V.; Tarasov, V.A.; Volkov, V.L. *Funct. Mat.* **2012**, *3*, 404-409. (c) Wright, G. T. *Proc. Phys. Soc. B* **1955**, *68*, 701-712.

(18) Nagano, Y.; Ikoma, T.; Akiyama, K.; Tero-Kubota, S. J. *Chem. Phys.* **2001**, *4*, 1775-1784.

(19) Wahadoszamen, M.; Hamada, T.; Iimori, T.; Nakabayashi, T.; Ohta, N. *J. Phys. Chem. A* **2007**, *111*, 9544-9552.

(20) Saltiel, J. ; Khalil, G.-E.; Schanze, K. *Chem. Phys. Lett.* **1980**, *2*, 233-235.

(21) Gorner, H. *J. Phys. Chem.* **1989**, *5*, 1826-1832.

(22) Ikeyama, T.; Azumi, T. *J. Phys. Chem.* **1985**, *89*, 5332-5333.

(23) Ciorba, S.; Clennan, E.L.; Mazzucato, U.; Spalletti, A.; *J. Lumin.* **2011**, *131*, 1193–1197.